Probing Confined Water with Nonphotochemical Hole Burning Spectroscopy: Aluminum Phthalocyanine Tetrasulfonate in Poly(2-hydroxyethyl methacrylate)†

N. C. Dang, T. Reinot, G. J. Small, and J. M. Hayes*

Department of Chemistry and Ames Laboratory-USDOE, Iowa State University, Ames, Iowa 50011

Received: February 26, 2003; In Final Form: June 18, 2003

Nonphotochemical hole burning is used to measure the linear electron−phonon coupling, the temperature dependence of the pure dephasing, and the zero-phonon hole growth kinetics of aluminum phthalocyanine tetrasulfonate (APT) in glassy water confined in pores (∼30 Å) of films of poly(2-hydroxyethyl methacrylate) (poly-HEMA). The hole burning properties of APT in the polymer are compared with those of APT in hyperquenched glassy films of water and ethanol. Below ∼8 K in the polymer, the dephasing, which is dominated by coupling to the intrinsic two-level systems (TLS_{int}) of the glass, is found to be more similar to that of APT in unannealed hyperquenched glassy water (HGW) films than in annealed HGW films. This shows, for the first time, that confinement does not lead to a significant decrease in the TLS_{int} density. At higher temperatures, dephasing due to exchange coupling with a pseudolocalized mode at 42 cm^{-1} becomes dominant. This coupling is due to diagonal quadratic electron−phonon coupling that leads to a change in mode energy upon electronic excitation of APT. The 42 cm^{-1} vibration is assigned to the transverse acoustic mode of confined water. In HGW the energy of this mode is 50 cm^{-1}. The interaction of APT with surface-bound water and the polymer surface also leads to reduction of the energy of the linearly coupled (Franck−Condon active) phonon mode from 38 cm^{-1} for HGW to 32 cm^{-1}. Hole growth kinetics measurements for APT in polymer saturated with D_2O are compared with those in polymer saturated with H_2O. In the heavy water the hole burning is 330 times slower. The equivalent factor for heavy HGW is 800. Thus, the mechanism of hole burning involves proton tunneling associated with the extrinsic two-level systems (TLS_{ext}) introduced by the dye. In contrast, dephasing data indicate that the coordinate of the TLS_{int} is spatially extended and involves only small-amplitude motion of protons. Differences between the hole-burning properties of APT in poly-HEMA and in HGW and hyperquenched ethanol are discussed in terms of the interactions of APT with bound (nonfreezable) water and the hydroxyethyl groups of the polymer.

I. Introduction

Recently, much attention has focused on the dynamical properties of water in confined spaces. Water in confined spaces differs in both structural and dynamic properties from bulk water. Understanding these differences is important for a variety of diverse areas. For example, protein structure and function are both often dependent on imbedded water.[1−3] Water-filled pores are often the channels through biological membranes.[4] Water in vesicles formed from block copolymers is important in developing drug delivery systems and for modeling of cell functions. Because of this importance, studies of water in a myriad of confined spaces are now widespread.

Dielectric relaxation and solvation dynamics of water in confined spaces have been recently reviewed by Nandi et al.[5] In that review, it is pointed out that water in cage-like hosts (e.g., cyclodextrans and calixirenes), microporous solids (e.g., zeolites), micelles, and semirigid materials (e.g., polymers and hydrogels) can serve as simpler surrogates for understanding the complex role of water in biological molecules (proteins and DNA). In all these varied media, the water can be divided into two types: free water with properties similar to those of unconfined, bulk water, and bound water that differs markedly from bulk water in its properties. Note that there is not always a sharp demarcation between these two types of water. In proteins and other biological macromolecules, the bound water is often referred to as biological water. Femtosecond solvation dynamics of biological water have been recently reviewed by Pal et al.[6]

Of interest here is the organic polymer, poly(2-hydroxyethyl methacrylate) (poly-HEMA). This is a water-absorbing polymer that can contain an equilibrium water content approaching 40%. The pore size of the polymer is ∼30 Å. A spherical cavity of this dimension would contain ∼500 water molecules.[7] Water in poly-HEMA is known to occupy two distinct environments. A portion of the water can crystallize at temperatures near the ice point of normal water and is referred to as freezable water. The freezable water can be identified as the unbound water described above. The remainder of the water, ∼44% of the total, does not crystallize.[8] This is called nonfreezable water and corresponds to the bound water. It is thought to constitute the layer of water in contact with the polymer inner surfaces that interacts with the polymer via hydrogen bonding. Note that bound water occupying 44% of the total volume of a spherical cavity of 30 Å diameter is found in a layer of <3 Å thickness. It is disruption of the normal water hydrogen bond network by polymer−water hydrogen bonds that prevents this water from freezing. Both water fractions can be vitrified but the T_g associated with each fraction is different. For the bound water, $T_g = 162$ K, while for the free water, $T_g = 132$ K.[9] The latter

† Part of the special issue "Charles S. Parmenter Festschrift".

* Corresponding author: jmhayes@iastate.edu.

10.1021/jp0344895 CCC: $25.00 © 2003 American Chemical Society
Published on Web 09/10/2003

value is similar to the T_g value for hyperquenched glassy water, HGW,[10] and is one indication that the free water has little interaction with the polymer and is akin to bulk water in its properties.

We report here the results of nonphotchemical hole-burning (NPHB) spectroscopic studies of aluminum phthalocyanine tetrasulfonate (APT) in water-soaked poly-HEMA. The current mechanism for NPHB is reviewed in ref 11. Suffice it to say that NPHB is a site excitation energy selective technique that eliminates the contribution from inhomogeneous broadening to the optical transitions of chromophores in amorphous hosts and that the mechanism of hole burning involves configurational tunneling of the chromophore/host system triggered by electronic excitation of the chromophore. Hole burning of APT in wet poly-HEMA was reported in ref 12. In that work, however, measurements were restricted to a single temperature, 4.5 K. Nevertheless, the results established that NPHB of APT is efficient, as had been found for APT in confined water in other porous materials,[13,14] and, furthermore, that the linear electron−phonon coupling of APT's $S_0 \rightarrow S_1$ (Q_x) transition in wet poly-HEMA differs significantly from that in hyperquenched glassy water (HGW). To further explore the effects of confined water on the spectral dynamics and hole-burning properties of APT we present pure dephasing data for the range 4−80 K and zero-phonon hole growth kinetics data obtained at 4.5 K. Growth kinetics data are also presented for heavy water (D_2O). The results are compared with those of APT in HGW. Importantly, it is found that the basic mechanism of pure dephasing for poly-HEMA and HGW are the same, that the hole growth kinetics for poly-HEMA are about as dispersive (distributed) as those for annealed HGW, and that the linear electron−phonon coupling for the two host systems are similar. However, some significant differences are observed and discussed in terms of the interactions of APT with bound (nonfreezable) water and the hydroxyethyl groups of the polymer.

II. Experimental Section

D_2O (Aldrich), poly-HEMA (Aldrich), and methanol (Fisher, 99.9%) were all used without further purification. Nanopure water ($R > 10$ MΩ cm^{-1}) was locally purified. Poly-HEMA (∼1 g) was dissolved in methanol (10 mL) by shaking. Several drops of this solution were dropped onto a glass coverslip and dried overnight in a covered container at 40 °C. Transparent films of ∼ 0.5 mm thickness, adherent to the glass substrate, were obtained. Residual solvent was removed by vacuum-drying at 40 °C for several hours. Before use, these samples were soaked in Nanopure water that was changed daily for 2 weeks.

To prepare the APT/poly-HEMA samples, the films described above were soaked in a 10^{-5} M APT in water solution for 24 h. Deuterated water samples were prepared similarly in a glovebag filled with dry nitrogen. The samples were mounted on a copper plate for cooling, with the polymer side facing the plate. Cooling was by immersion into liquid helium. The cooling rate is estimated to be 0.5 K s^{-1}. Temperature was measured with a DT-470 silicon diode (Lakeshore, Inc.) also mounted in contact with the copper plate.

The laser system used for hole burning and measuring fluorescence excitation spectra has been described in detail elsewhere.[15,16] In brief, the laser system is a Coherent 699-29 ring dye laser (DCM or LD 688 dye, line width < 10 MHz) pumped by a Coherent Innova argon ion laser (6 W, all lines). The laser intensity was regulated with an electrooptic beam stabilizer (Cambridge Research and Instrumentation, LS100). A beam expander and neutral density filters were used to adjust the power density at the sample. Fluorescence from the sample was filtered by a long pass filter (Omega Optical, AELP-730) and detected by a Hamamatsu R-2949 photomultiplier tube followed by a photon counter (Stanford Research, SR400). Fluorescence excitation spectra were recorded with a resolution of 20 MHz for the low temperature (<25 K) data and 0.4 cm^{-1} at higher temperatures. Care was taken to ensure that the laser intensities used to read spectra were low enough to prevent hole burning during reading. Hole growth kinetics were measured by monitoring the fluorescence intensity as a function of time.

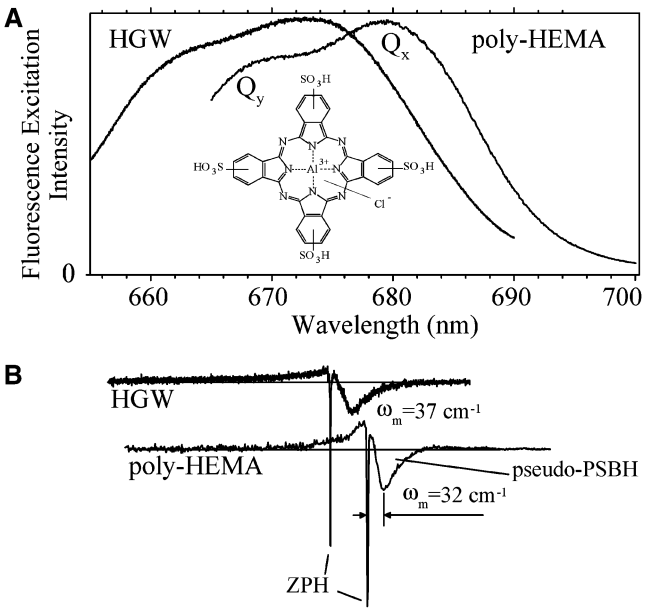

Figure 1. (A) Fluorescence excitation spectra of APT in HGW (T = 5 K) and in water-saturated poly-HEMA (T = 4.5 K). The chemical structure for APT is shown, also. (B) Hole spectra for APT in HGW and in water-saturated poly-HEMA. The spectra in B are on the same wavelength scale as in (A).

TABLE 1: Q_x Transition Energies, Q_x–Q_y Splittings, and Peak Phonon Frequencies for APT in Various Glasses[a]

	Q_x, cm^{-1}	ΔQ_{xy}, cm^{-1}	ω_m, cm^{-1}
dry poly-HEMA[b]	14 650	340	25
wet poly-HEMA[b]	14 700	260	32
HGW	14 910[c]	230[c]	38[d]
HGE	14 700[c]	180[c]	26[d]
HGM	14 740[c]	190[c]	17[d]

[a] At room temperature, the Q_x transition energies are 14 831, 14 718, and 14 696 cm^{-1} for water, ethanol, and methanol, respectively. [b] From ref 9. [c] From ref 12. [d] From ref 25.

III. Results

Fluorescence excitation spectra of APT in HGW at 5 K and in poly-HEMA at 4.5 K are compared in Figure 1. The structure of the dye molecule is included as an inset in the figure. Note that in either matrix, the APT absorption consists of two broad, unresolved bands. Previously, it has been shown that these two bands are the Q_x and Q_y transitions of the molecule.[17] In ref 17, it was demonstrated that the Q-band transition of APT, which is expected to be degenerate based on molecular symmetry, is split by the binding of two water molecules to the aluminum atom. Note that the APT/ poly-HEMA absorption is red-shifted 6.5 nm (210 cm^{-1}) relative to that of APT/ HGW. Q_x transition energies for APT in several glasses are listed in Table 1.

The lower panel of Figure 1 shows two medium fluence holes burned into the APT Q_x absorption. The upper hole spectrum

TABLE 2: Dephasing Parameters for APT in Various Matrices

	a, cm^{-1}	b_1, cm^{-1}	b_2, cm^{-1}	ω_1, cm^{-1}	ω_2, cm^{-1}	α	τ_1, ps	τ_2, ps
HGW, annealed[a]	0.0002	6.9	11.1	50	182	1.3	1.5	1.0
HGW fresh[a]	0.0010	7.0	53	53	179	1.3	1.5	0.2
wet p-HEMA	0.0018	2.6		42		1.3	4.1	

[a] From ref 16. Fresh HGW refers to a film deposited at $T \approx 5$ K, while annealed refers to a film which is warmed to a temperature near T_g before cooling to the measurement temperature.

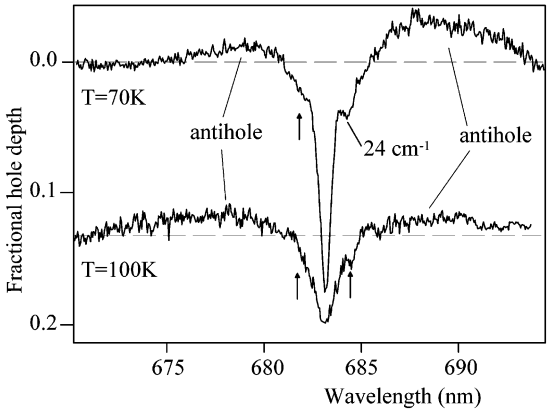

Figure 2. Hole spectra for APT in water-saturated poly-HEMA. The upper spectrum was burned and detected at 70 K, while the lower spectrum was burned and detected at 100 K. Vertical arrows are displaced ± 24 cm^{-1} from the burn wavelength and mark the real phonon and pseudo-phonon sideband holes.

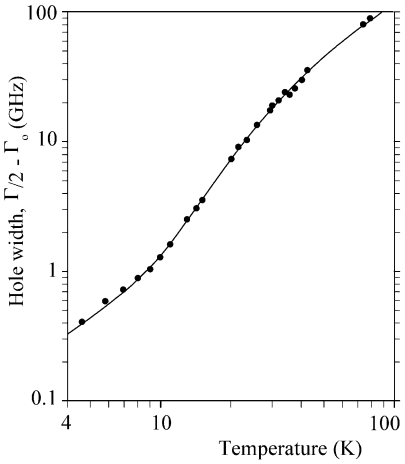

Figure 3. Temperature dependence of the ZPH width for APT in water-saturated poly-HEMA. The data points were measured as described in the text. The solid line is the fit to eq 1.

is for APT in HGW, while the lower spectrum is for APT/poly-HEMA. The holes shown were burned at 675.0 nm for APT/HGW and at 685.0 nm for APT/poly-HEMA. In the figure, the zero-phonon hole (ZPH) in poly-HEMA appears slightly broader than in HGW. For both samples, the ZPH are fluence broadened to some extent. At 5 K, for annealed HGW, the ZPH width can be as narrow as 110 MHz, while for fresh APT/HGW, the width is 550 MHz. In poly-HEMA at 4.5 K, the ZPH width is 900 MHz. Note that the peak phonon frequencies, ω_m, associated with the pseudo-phonon sideband hole (pseudo-PSBH) differ for the two samples. The high value of ω_m (37 cm^{-1}) for APT/HGW is in large measure responsible for being able to resolve ZPH in HGW up to almost T_g. For APT/poly-HEMA, the lower value of ω_m (32 cm^{-1}) results in a smaller range over which the ZPH can be resolved from phonon sideband holes, restricting the ZPH width measurements. Nevertheless, 32 cm^{-1} is significantly larger than values of $\omega_m < 25$ cm^{-1} common in many non-water-containing polymer/dye systems.[18] One final point regarding the two hole spectra is that the antihole (positive absorption increase to the blue of the ZPH) is more prominent for the poly-HEMA sample. This in part is due to the increased integrated hole area of the poly-HEMA ZPH but more importantly is due to a narrower antihole site distribution.

Hole widths were measured from fitting Lorentzians to the ZPH of a series of holes burned a few gigahertz apart at a burn temperature, T_B. After measuring those holes, the temperature was raised and the holes were remeasured. This continued until the holes were too shallow to measure accurately. At this point, a new set of holes was burned at a higher T_B and the process continued. In the course of the measurements, it was verified that the widths measured at some temperature, T, above T_B, were the same as the width of a hole burned at T, if the holes were burned with the same fluence. At 70 K and above, as shown in Figure 2, although it was still possible to detect the hole, the ZPH was not well-resolved from the accompanying pseudo- and real-phonon sideband holes (indicated by the arrows in the figure). However, it was still possible to measure the ZPH width with reasonable accuracy up to ~80 K. At higher temperatures, the overlap between ZPH and sideband holes prevented accurate measurement. See, for example, the $T_B = 100$ K hole profile in Figure 2, where the real PSBH and pseudo-PSBH are indicated by arrows.

Hole widths, expressed as $\Gamma_h/2 - \Gamma_0$, are plotted versus temperature in Figure 3. Here, Γ_h is the measured hole width and Γ_0 is the lifetime limited line width of the zero-phonon line, $\Gamma_0 = 1/(2\pi\tau_{fl}) = 25$ MHz. The fluorescence lifetime (τ_{fl}) was measured as 6.5 ns at 77 K for HGW deposited at 77 K. At temperatures < 25 K, the hole widths are determined by extrapolating the hole widths at several fluences to the zero fluence value. Above 25 K, the values shown are the narrowest value recorded at each temperature. The solid line is a fit to the data by using the expression

$$\Gamma_h/2 - \Gamma_0 = aT^\alpha + b\bar{n}(\omega) \qquad (1)$$

which follows in the slow modulation limit of exchange coupling in the Jackson-Silbey theory.[19] The first term in eq 1 describes dephasing from coupling of the electronic transition to the intrinsic two-level systems (TLS_{int}) of the glass host. The TLS_{int} correspond to bistable intermolecular potentials.[20] For a wide variety of probe molecules in amorphous hosts, $\alpha \approx 1.3$,[21,22] as is also found here; see Table 2. This term dominates the low-temperature dephasing ($T < 8$ K), while the second term is associated with dephasing due to exchange coupling with a pseudo-localized phonon, of frequency ω. $\bar{n}(\omega)$ is the thermal occupation number of the mode. The phonon relaxation time (τ) is given in the low-temperature limit by $(bc\pi)^{-1}$ with $c = 3 \times 10^{10}$ cm s^{-1}.[21] Values obtained from fitting eq 1 to the hole width data are given in Table 2.

Figure 4 compares hole burning for APT in water-saturated poly-HEMA to hole burning of APT/poly-HEMA in which the polymer was saturated with a solution of APT in D_2O. The hole spectra shown for the two samples are quite similar. However, the spectra were burned with significantly different fluences.

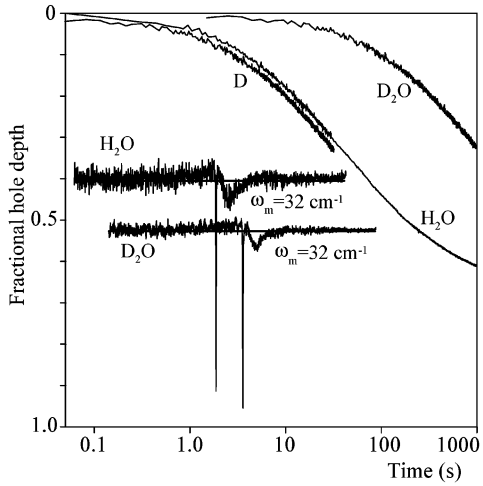

Figure 4. Hole growth kinetics for APT in H_2O- and D_2O-saturated poly-HEMA. Curve D is the D_2O data with time axis compressed 15-fold and slightly shifted along the ordinate so as not to obscure the H_2O curve. Also shown are the saturated hole spectra for APT in the two samples. The hole spectra were burned at the same wavelength (689 nm) but have been shifted for clarity. Burn fluence was 1.5 J cm^{-2} for D_2O and 6 mJ cm^{-2} for H_2O; $T = 4.5$ K.

For the deuterated sample, a burn intensity of 50 mW cm^{-2} was used, while for the protonated sample the burn intensity was 0.2 mW cm^{-2}. For both samples, the burn time was 30 s. This difference in burn rates is reflected in the hole growth kinetics curves, labeled H_2O and D_2O in the figure. As is commonly observed for NPHB, the growth rates are nonexponential.[23] This is primarily due to a distribution of tunneling rates for the TLS_{ext} involved in the hole-burning process.[23,24] Curve D in the figure is the D_2O curve with the time axis compressed by a factor of 15. This compression results in the D_2O and H_2O curves overlapping, exactly. (The D_2O curve is shifted slightly along the ordinate for clarity.) However, the D_2O growth curve was obtained with a power density of 15 μW cm^{-2} and the H_2O growth curve with 0.7 μW cm^{-2}. Based on the burn intensity difference and the 15× compression factor, the D_2O sample burns ~320 times slower than the H_2O sample.

IV. Discussion

A. Transition Energies and Q_x–Q_y Splittings. As can be seen in Figure 1A, the fluorescence excitation spectrum of APT in poly-HEMA is red-shifted from the corresponding spectrum for APT in HGW. In Table 1 are shown the low-temperature Q_x transition energies for APT in several glasses as measured from the fluorescence excitation spectra. The room-temperature values for the corresponding liquids as measured from absorption spectra are given in the caption. The Q_x–Q_y splittings (ΔQ_{xy}) and the peak phonon frequencies (ω_m) as determined from hole spectra of APT in those glasses are also tabulated. From the table, it can be seen that APT in wet poly-HEMA has a Q_x energy similar to that of APT in HGE, while for dry poly-HEMA the absorption is further red-shifted.

Before discussing the poly-HEMA data, it is instructive to compare the data from Table 1 for the liquids and their hyperquenched glasses. Consider first the values for ΔQ_{xy} (uncertainty of ± 15 cm^{-1}). The value of 230 cm^{-1} for HGW is close to the value of 215 cm^{-1} determined from molecular mechanics and ZINDO calculations.[17] This value is for two water molecules ligated to the central aluminum of APT and oriented with the water hydrogens aligned with the bridging nitrogens and the two water molecules (on opposite sides of the macrocycle) so as to preserve the σ_h symmetry plane. It is this structure that gives the maximum values for ΔQ_{xy}. The value for hyperquenched glassy ethanol (HGE) and hyperquenched glassy methanol (HGM) are somewhat lower than the value for HGW. As discussed in ref 25, similar values for the three glasses are expected since the ethanol and methanol contain ~1% water. That is, water molecules are expected to be ligated to the central aluminum in methanol and ethanol. Hydrogen bonding between the ligated water and ethanol (methanol) molecules would be expected to have some effect on ΔQ_{xy}. The significant difference between the frequencies (ω_m) of the Franck−Condon active phonons for the three glasses are consistent with such hydrogen bonding, vide infra.

Consider next the Q_x transition energies. At room temperature, the energies in methanol and ethanol are nearly identical, while water is blue-shifted ~100 cm^{-1}. In ref 26 it was estimated on the basis of a pressure-dependent study of the zero-phonon holes of APT in HGW that the Q_x transition of APT in the gas phase is at roughly 15 000 cm^{-1}. Thus, the solution values for the Q_x transition of ethanol and methanol are red-shifted from the vapor value. The situation for water is less clear. Upon the formation of HGE, the Q_x transition barely changes, while HGW and HGM undergo a blue shift. Given that the permanent dipole change of APT's $S_0 \rightarrow Q_x$ transition is very small, <0.1 D as determined by Stark hole-burning spectroscopy, it seems unlikely that dipole (solvent)−induced dipole (APT) interactions make a significant contribution to the solvent shifts.[27] It is likely that dispersion and hydrogen bonding interactions are the major contributors to the solvent shifts. The results are consistent with hydrogen bonding in water and HGW being stronger than in methanol (HGM) and ethanol (HGE) and, furthermore, they are consistent with hydrogen bonding resulting in a blue shift of the of the Q_x transition in going from the vapor to the condensed phase. This is in line with the observation that formation of HGW from water results in a blue shift. Since dispersion interactions are expected to result in red-shifting,[28] it appears that in methanol (HGM) and ethanol (HGE) they dominate the hydrogen bonding interactions, while the opposite is true for water (HGW).

The phonon frequencies (ω_m) in Table 1 provide some support for this. In ref 25 it was proposed that Franck−Condon active phonons in the hole spectra most likely represent librational motions of APT hydrogen bonded to the glass network. Thus, one expects ω_m of HGW (38 cm^{-1}) to be higher than the value for HGM and HGE, as is observed. However, it is not apparent why the value of 17 cm^{-1} for HGM is significantly lower than the value of 26 cm^{-1} for HGE. MM/QM calculations might shed light on this.

Turning now to the values for APT in wet poly-HEMA (Table 1), the evidence seems to indicate that the APT is located such that it interacts both with the nonfreezable water and with the hydroxyethyl groups that line the polymer pores. In ref 12 it was proposed that APT in poly-HEMA must be located at least partially in contact with the nonfreezable (bound) water based on two factors: that hole burning of APT did not cease after annealing the sample above the crystallization temperature of the freezable water and that the APT dimensions would require the molecule to be nearly perfectly centered in a pore to avoid interaction with the bound water and hydroxyethyl groups. In HGW, it has been reported that hole burning ceases after the sample is annealed at temperatures sufficient to cause transformation of the HGW to cubic ice.[15] This is also as expected from the current understanding of the NPHB mechanism.[29,11] Based on the size of APT (20 Å lateral dimension) compared to the average poly-HEMA pore size (30 Å diameter) some

interaction between APT and bound water and the hydroxyethyl groups of the polymer is expected. Given the size of APT, it is possible that APT prevents crystallization of the freezable water in the pores.

Regarding the values of ΔQ_{xy} for the polymers, the large splitting in the wet polymer is puzzling, as it is expected that two water molecules are still ligated to the aluminum in this sample. The larger splitting here must reflect, to some extent, interactions between APT and bound water and the hydroxyethyl groups. Interestingly, the ΔQ_{xy} splitting and red-shift of the Q_x transition for dry poly-HEMA are the largest for all the systems studied. The drying procedure is expected to remove freezable and bound water from the pores. However, the Al-ligated water may not have been removed. The large red-shift is most likely due to weakening of hydrogen bond interactions between the host medium and APT due to removal of most of the water molecules. Again, hydrogen bonding leads to blue-shifting of the Q_x-transition. The low value of 25 cm^{-1} for ω_m is consistent with this. The large ΔQ_{xy} value of 340 cm^{-1} may be due to collapse of the polymer about APT that occurs upon drying. This collapse could conceivably result in an APT structure that is different from that in the three glasses and in wet poly-HEMA.

B. Temperature Dependence of Pure Dephasing of APT in Wet Poly-HEMA. The temperature dependence of the dephasing is shown in Figure 3. The solid line is a fit to the experimental data, using eq 1. The values of the fitting parameters are given in Table 2 along with the corresponding data for APT in fresh and annealed HGW.[16] The first term of eq 1 describes dephasing due to diagonal modulation associated with the electron$-TLS_{int}$ interaction. At temperatures $\lesssim$8 K, this term dominates the dephasing. For molecular systems, α is typically 1.3, as previously reported for APT/HGW[16] and as found here for APT/poly-HEMA. The $b\bar{n}(\omega)$ form for the exchange coupling applies in the slow modulation limit, $\delta < \tau^{-1}$, where δ is the difference in frequency of the pseudo-local mode for the ground and excited electronic states of the probe and τ^{-1}, the relaxation frequency, is given by

$$\tau^{-1}(T) = 2\pi g(\omega) D(\omega)[\bar{n}(\omega) + 1] \qquad (2)$$

Here ω is the effective frequency of the pseudo-local mode, $g(\omega)$ is the density of states of modes which couple to the pseudo-local mode, and $D(\omega)$ is the coupling function. In the slow modulation limit, $\tau(0\ K) = (bc\pi)^{-1}$, where b is in cm^{-1} and c is the speed of light. For APT in wet poly-HEMA, $\tau(0\ K) = 4.1$ ps. The corresponding value for APT/HGW is 1.5 ps. Whether or not the longer lifetime in poly-HEMA is due to a decrease in the value of $g(\omega)$ or a decrease in $D(\omega)$ or a combination of both is unclear.

From Table 2, note that the electron-TLS_{int} dephasing for poly-HEMA is similar to that of APT in fresh HGW. In HGW, the ZPH width at 5 K decreases by a factor of 5 if the sample is annealed at $\sim$130 K.[15] This width decrease is indicative of a 5-fold decrease of the density of TLS_{int} in the sample.[15] This TLS_{int} density decrease is mirrored in the amplitude of the TLS_{int}-electron dephasing term, which also decreases 5$\times$ on annealing. For the poly-HEMA sample, annealing of a quickly cooled sample does result in a decrease in the ZPH width.[12] However, in the present work, the samples were slowly cooled and the initial widths at 5 K were comparable to those reported for annealed samples in ref 12. Comparing the amplitude of the TLS-electron dephasing for poly-HEMA and fresh HGW, the values differ by somewhat less than a factor of 2, while the ZPH widths at 5 K are a factor of 2 different, vide infra. An important point is that the TLS_{int}'s that dictate pure dephasing in bulk glasses at low temperatures also exist in confined glassy solids and are active in dephasing. It seems likely, however, that the bound water is involved in the structures of at least a fraction of the TLS_{int}.

Note that for APT/HGW, as described in ref 16, two phonon modes at 53 and 180 cm^{-1} were used to fit the dephasing data over the range from 5 to 100 K, although only a single mode at 53 cm^{-1} was sufficient up to 70 K. In the case of APT/poly-HEMA, the data are only available up to 80 K, and here also only a single mode with energy 42 cm^{-1} is needed to obtain a good fit.

As in the case of APT/HGW and also APT in HGE,[25] the pseudo-local mode active in dephasing differs in frequency from the mode that appears (as a phonon sideband hole) in the hole spectra. As pointed out in ref 16, the phonon sideband hole arises due to linear electron$-$phonon coupling (with coupling strength given by the Huang$-$Rhys factor, S), while the mode causing dephasing through the exchange mechanism occurs via diagonal quadratic electron$-$phonon coupling. For HGW, the two modes (53 and 180 cm^{-1}) needed to fit the dephasing data can be identified with known modes of liquid water. Although the dynamical nature of these modes is the subject of current research, there appears to be general agreement that they are acoustic (translational) in nature. Walrafen[30] assigns the 50 and 180 cm^{-1} modes as transverse (shear-like) and longitudinal (dilational) in character, respectively, with the latter corresponding to O$-$O stretching of O$-$H$\cdot\cdot$O units in a T_d arrangement (in a time-averaged sense). Shear motion of two water molecules leads to O$-$O$-$O bending and center of mass motion. Both modes are viewed as standing waves associated with hydrogen-bonded structures whose spatial extent in the glass is expected to be limited because of structural disorder.

For ethanol, only a single mode (47 cm^{-1}) was needed to fit the dephasing data. The similarity between the HGW and HGE mode frequencies, together with similar values for the maxima in spectral densities of the two liquids, and similar vibrational dynamics suggest an identification of the exchange coupled modes with the spectral density maxima.[25] In contrast, the phonon sideband frequencies for APT in HGW and in HGE are not similar (37 cm^{-1} in HGW and 26 cm^{-1} in HGE), showing that the linearly coupled modes cannot be identified with the quadratically coupled modes. In ref 25 it was proposed that the phonon sideband mode is a libration of APT with the differences in mode frequencies for HGW and HGE reflecting difference in hydrogen bonding strength in the two glasses.

With reference to APT/wet poly-HEMA, by analogy with HGW, the 42 cm^{-1} mode causing dephasing would be expected to show up as a maximum in the spectral density for water-saturated poly-HEMA. The reduction from the water value of $\sim$50 cm^{-1} then is indicative of the disruption of the water structure in the polymer relative to bulk water. The mode at 32 cm^{-1} observed as a phonon sideband hole is also most likely due to APT libration with a frequency between the mode frequency of HGW and HGE indicating that the average hydrogen bonding to APT in wet poly-HEMA is weaker than in HGW but stronger than in HGE.

C. Dispersive Hole Growth Kinetics of APT in Wet Poly-HEMA. Further evidence for the structure of glassy water about APT in poly-HEMA being a disrupted form of the APT environment in HGW comes from the deuteration data shown in Figure 4. As has often been observed, deuteration of the host in NPHB does not effect the ZPH width or phonon frequency but does greatly decrease the hole-burning efficiency.[20] The absence of a deuteration effect on hole widths indicates that

TABLE 3: Hole Growth Kinetics Parameters for APT in Wet Poly-HEMA and in HGW[a]

	S	λ_0	σ_λ	$\langle\varphi\rangle$	$\langle R\rangle$, s^{-1}
protonated HGW[b] (fresh/annealed)	0.55	8.2/8.3	1.3/0.9	0.78/0.015	$1.3 \times 10^7/2.4 \times 10^6$
deuterated HGW (fresh/annealed)	0.60	11.0/11.0	1.0/0.85	$1.4 \times 10^{-4}/8.2 \times 10^{-5}$	$1.6 \times 10^4/9.0 \times 10^3$
wet p-HEMA, protonated	0.44	9.2	0.8	0.0048	2.8×10^5
HT	0.55	12.1	0.8	7.7×10^{-6}	8.4×10^2

[a] From ref 31. [b] Lower values of S, λ_0, and σ_λ, for protonated HGW, were reported in ref 11. The values listed here from ref 31 were determined by a method similar to that used for the poly-HEMA measurements.

the TLS_{int} are spatially extended with only small-amplitude proton motion.[22] However, the rate-determining step in NPHB involves extrinsic two-level systems associated with the probe and its inner shell of host molecules and large-amplitude proton motion.[29] As shown in the figure, a 15× time compression of the data for the deuterated sample results in coincidence of the deuterated and protonated results. Taking into consideration the difference in burn fluences used for the two samples, the deuterated sample burns 320 times slower than the protonated sample.

The kinetics data were fit by the expression[24]

$$D(t) = 1.5\int d\lambda f(\lambda)\int d\alpha \sin\alpha \cos^2\alpha e^{-P\sigma_{LT}{}^p\phi(\lambda)\cos^2\alpha t} \quad (3)$$

In this equation, $D(t)$ is the fluorescence excitation signal at holeburning time, t, λ is the tunnel parameter for TLS_{ext}, $f(\lambda)$ is its Gaussian distribution function centered at λ_o with standard deviation σ_λ, α is the angle between burn laser polarization and the transition dipole, P is the photon flux in number of photons cm^{-2} s^{-1}, $\sigma_{LT}{}^p$ is the peak absorption cross section at low temperature (5.5×10^{-11} cm^2), and $\phi(\lambda)$ is the NPHB quantum yield given by

$$\phi(\lambda) = \frac{\Omega_0 \exp(-2\lambda)}{\Omega_0 \exp(-2\lambda) + \tau_{fl}{}^{-1}} \quad (4)$$

In eq 4, τ_{fl} is the fluorescence lifetime and Ω_0 is the prefactor in the Fermi Golden rule expression for the TLS relaxation rate for nonphotochemical hole burning, $R = \Omega_0 \exp(-2\lambda)$.[22] As in refs 15 and 31, a value of 7.6×10^{12} s^{-1} was used for Ω_0. In fitting data using eq 3, the data must be scaled with the Huang−Rhys factor, S, which limits the maximum ZPH depth to $\exp(-S)$.[23] Thus, the fractional ZPH depth, $d(t)$, is given by $d(t) = (1 - D(t))e^{-S}$. The parameters resulting from fitting the protonated and deuterated data of Figure 4 are given in Table 3, along with the corresponding data for APT in protonated and deuterated HGW.

In Table 3, the values $\langle R\rangle$ and $\langle\phi\rangle$ are the average TLS tunneling rate, $\langle R\rangle = \Omega_0 \exp(-2\lambda_0) \exp(2\sigma_\lambda{}^2)$, and the average quantum yield for hole burning, $\langle\phi\rangle = \langle R\rangle/(\langle R\rangle + \tau_{fl}{}^{-1})$, respectively. The ratio of the values of $\langle R\rangle$ for the deuterated and protonated poly-HEMA samples is ∼330, nearly the same as determined from curve D of Figure 4. The ratio of $\langle\phi\rangle$ for the protonated and deuterated samples is not the same because the two fluorescence lifetimes differ. As stated previously, fluorescence lifetimes were determined for APT in HGW and deuterated HGW at 77 K. In protonated HGW, $\tau_{fl} = 6.5$ ns, while in deuterated HGW, $\tau_{fl} = 9.2$ ns. These values were used for fitting the hole growth kinetics curves in HGW and in poly-HEMA. The ratio of $\langle R\rangle$ values for HGW, protonated and deuterated, is ∼800, a little more than twice the value for poly-HEMA. A factor of ∼2 difference between poly-HEMA and fresh HGW was also noted in the low-temperature dephasing data. However, in contrast to the dephasing data for which poly-HEMA seems to be similar to fresh HGW films, the values of λ_0 and σ_λ for poly-HEMA are more like the values for annealed HGW. Note that while the dephasing data are dependent on the density of states of TLS_{int}, the kinetics parameters reflect the tunneling rate for TLS_{ext}. Thus, although the TLS_{int} density of states for poly-HEMA is similar to that of fresh HGW, the inner solvent shell around the APT molecule appears to be as highly ordered as it is in annealed HGW. Comparing the λ_0 and σ_λ values for protonated and deuterated poly-HEMA, note that the σ_λ values are the same while the λ_0 values are different. The ratio of $\lambda_0{}^D/\lambda_0{}^H$ is 1.3, the same as for the HGW ratio and nearly equal to the isotopic mass ratio $\sqrt{2}$, which indicates that it is proton tunneling that is involved in the TLS_{ext}.

V. Concluding Remarks

As discussed in the Introduction, understanding of the properties of water in confined spaces is an important step toward understanding the role and properties of water in biological systems. Here, spectral hole burning has been used to probe the environment of the APT chromophore confined to the pores of the poly-HEMA polymer. These pores are lined with hydroxyethyl groups and are water-filled. Thus, the hole-burning properties of the APT−water−polymer system were compared to the hole-burning properties of HGW and of HGE. From this comparison, it is concluded that the APT molecule is located so that it interacts with both the bound (unfreezable) water and with the hydroxyethyl groups.

The results presented further establish that nonphotochemical hole burning (NPHB) can be used to distinguish between a probe molecule in confined and bulk glassy environments. The properties of aluminum phthalocyanine tetrasulfonate (APT) in wet poly-HEMA films (pore size ∼30 Å) investigated include (1) T dependence of pure dephasing due to electron−TLS coupling and quadratic electron−phonon coupling, (2) the linear electron−phonon coupling (Huang−Rhys factor S and peak phonon frequency ω_m) that results in phonon sideband hole structure, (3) zero-phonon hole growth kinetics, and (4) the energy of APT's $S_0 \rightarrow S_1$ origin transition. The results were compared with those of APT in bulk hyperquenched glassy water (HGW, fresh and annealed), APT in bulk hyperquenched glasses of ethanol (HGE), and APT in "dry" poly-HEMA. Concerning (1), the basic mechanisms of dephasing in poly-HEMA are the same as in HGW with electron−TLS_{int} coupling dominating the dephasing below 8 K. At higher temperatures the dephasing in poly-HEMA is dominated by quadratic electron−phonon coupling to a 42 cm^{-1} mode that correlates with the active 50 cm^{-1} mode in HGW. The latter had been assigned to the transverse acoustic mode of glassy water. It is not clear if the decrease to 42 cm^{-1} is entirely due to the effects of the bound water and hydroxyethyl groups of the pore surface. That is, APT with its 20 Å lateral dimension might also affect the acoustic mode energy of the freezable (unbound) water. Concerning (2), $\omega_m = 32$ cm^{-1} for wet poly-HEMA, compared with values of 38 and 26 cm^{-1} for HGW and HGE, respectively. The intermediate value of 32 cm^{-1} suggests that APT interacts to some degree with the hydroxyethyl groups. That the value

of $\omega_m = 25\ cm^{-1}$ for dry poly-HEMA and that the Q_x transition energy of APT in wet poly-HEMA is equal to that in HGE provide support for interactions with the hydroxyethyl groups. Comparison of the Q_x transition energies of the systems studied indicates that H-bonding with APT, which is strongest for water, leads to a blue-shifting of the Q_x state that counteracts the red-shifting due to dispersion interactions.

As discussed herein, the APT/poly-HEMA system does not possess hole-burning properties (ZPH width, Huang−Rhys factor, mean phonon frequency) as well suited to hole burning at higher temperatures as the APT/HGW system. Nevertheless, ZPH in the polymer system can be resolved up to 80 K. APT in other matrixes containing confined water has previously been studied both by hole burning[13,14] and by fluorescence line narrowing spectroscopy.[32] Galaup and co-workers have studied APT in water confined in the pores of a xerogel and in a porous glass (Vycor).[13,14] In the Vycor matrix, ZPH was detectable up to 80 K.[14] That system was characterized by a peak phonon frequency of 32 cm^{-1} and a Huang−Rhys factor of 0.13. However, the reported 80 K hole width was 9−10 cm^{-1}, while for APT/ poly-HEMA the 80 K width is ∼7 cm^{-1}. In the APT/ xerogel studied in that work, the phonon frequency was 25 cm^{-1} and the Huang−Rhys factor was 0.26. In the xerogel, ZPH was not detectable above 60 K. APT in a poly(acrylamide) gel was studied by Saikan and co-workers by fluorescence line narrowing spectroscopy.[32] For that polymer, zero phonon lines in emission were measurable up to 110 K. For the hydrolyzed gel, the phonon frequency was 38 cm^{-1}. Although a Huang−Rhys factor was not reported, the electron−phonon coupling was described as weak.

Note Added after ASAP Posting. This article was posted ASAP on 9/10/2003. Reference numbers in the footnotes of Tables 1, 2, and 3 have been changed. The correct version was posted on 11/6/2003.

References and Notes

(1) Bhattacharyya, K.; Bagchi, B. *J. Phys. Chem. A* **2000**, *104*, 10 603.
(2) Crupi, V.; Majolino, D.; Migliardo, P.; Venuti, V. *J. Phys. Chem. A* **2000**, *104*, 11 000.
(3) Bellisent-Funel, M. C. *J. Phys.-Condens. Matter* **2001**, *13*, 9165.
(4) Beckstein, O.; Biggin, P. C.; Sansom, M. S. P. *J. Phys. Chem. B* **2001**, *105*, 12 902.
(5) Nandi, N.; Bhattacharyya, K.; Bagchi, B. *Chem. Rev.* **2000**, *100*, 2013.
(6) Pal, S. K.; Peon, J.; Bagchi, B.; Zewail, A. H. *J. Phys. Chem. B* **2002**, *106*, 12 376.
(7) Pathmanathan, K.; Johari, G. P. *J. Polym. Sci. B, Polym. Phys.* **1990**, *28*, 675.
(8) Corkhill, P. H.; Jolly, A. M.; Ng, C. O.; Tighe, B. J. *Polymer* **1987**, *28*, 1760.
(9) Hofer, K.; Mayer, E.; Johari, G. P. *J. Phys. Chem.* **1990**, *94*, 2689.
(10) Hallbrucker, A.; Mayer, E.; Johari, G. P. *J. Phys. Chem.* **1989**, *93*, 7751.
(11) Reinot, T.; Small, G. J. *J. Chem. Phys.* **2001**, *114*, 9105.
(12) Hayes, J. M.; Reinot, T.; Small, G. J. *Chem. Phys. Lett.* **1999**, *312*, 362.
(13) Galaup, J.-P.; Fraigne, S.; Landraud, N.; Chaput, F.; Boilot, J.-P. *J. Luminesc.* **2001**, *94*−*95*, 719.
(14) Galaup, J.-P.; Fraigne, S.; Landraud, N.; Chaput, F.; Boilot, J.-P. *J. Luminesc.* **2002**, *98*, 189.
(15) Kim, W.-H.; Reinot, T.; Hayes, J.; Small, G. J. *J. Phys. Chem.* **1995**, *99*, 7300.
(16) Reinot, T.; Kim, W.-H.; Hayes, J. M.; Small, G. J. *J. Chem. Phys.* **1996**, *104*, 793.
(17) Reinot, T.; Hayes, J. M.; Small, G. J.; Zerner, M. C. *Chem. Phys. Lett.* **1999**, *299*, 410.
(18) Furusawa, A.; Horie, K.; Mita, I. *Japan, J. Appl. Phys.* **1989**, *28*, Suppl. 28−3, 247.
(19) Jackson, B.; Silbey, R. *Chem. Phys. Lett.* **1983**, *99*, 331.
(20) Jankowiak, R.; Hayes, J. M.; Small, G. J. *Chem. Rev.* **1993**, *93*, 1471.
(21) Völker, S. in *Relaxation Processes in Molecular Excited States*; Funfschilling, J., Ed.; Kluwer: Dordrecht, 1989; p 113.
(22) Narasimhan, L. R.; Littau, K. A.; Pack, D. W.; Bai, Y. S.; Elschner, A.; Fayer, M. D. *Chem. Rev.* **1990**, *90*, 439.
(23) Kenney, M. J.; Jankowiak, R.; Small, G. J. *Chem Phys.* **1990**, *146*, 47.
(24) Reinot, T.; Dang, N.; Small, G. J. *J. Luminesc.* **2002**, *98*, 183.
(25) Reinot, T.; Hayes, J. M.; Small, G. J. *J. Chem. Phys.* **1997**, *106*, 457.
(26) Hayes, J. M.; Reinot, T.; Shields, P.; Small, G. J. *Rev. Sci. Instrum.* **1999**, *70*, 2455.
(27) Reinot, T. *unpublished results*.
(28) McRae, E. G. *J. Phys. Chem.* **1957**, *61*, 562.
(29) Shu, L.; Small, G. J. *J. Opt. Soc. Am. B* **1992**, *9*, 724.
(30) Walrafen, G. E. *J. Phys. Chem.* **1990**, *94*, 2237.
(31) Kim, W.-H.; Reinot, T.; Hayes, J. M.; Small, G. J. *J. Chem. Phys.* **1996**, *104*, 6415.
(32) Mikami, M.; Ueta, T.; Kobayashi, D.; Koreeda, A.; Saikan, S. *J. Luminesc.* **2000**, *86*, 257.